Inorg. Chem. **2006**, *45*, 10263–10269

Computational Study of Iron(II) and -(III) Complexes with a Simple Model Human H Ferritin Ferroxidase Center

Daniel E. Bacelo[†,‡] and R. C. Binning Jr.*[,†]

Department of Sciences and Technology, Universidad Metropolitana, P. O. Box 21150, San Juan, Puerto Rico 00928-1150, and Departmento de Química, FCN, Universidad Nacional de la Patagonia San Juan Bosco, Km. 4, (9000) Comodoro Rivadavia, Chubut, Argentina

Received March 8, 2006

Interaction of iron ions with a six-amino acid model of the ferroxidase center of human H chain ferritin has been examined in density functional theory calculations. The model, based on experimental studies of oxidation of Fe^{2+} at the center, consists of Glu27, Glu62, His65, Glu107, Gln141, and Ala144. Reasonable structures are obtained in a survey of types of iron complexes inferred to occur in the ferroxidase reaction. Structures of complexes of the model center with one and two Fe^{2+} ions, with diiron(III) bridged by peroxide and bridged by oxide–peroxide combinations, have been optimized. Calculations on diiron(III) complexes confirm that stable peroxide-bridged complexes can form and that the Fe–Fe distance in at least one is consistent with the experimental Fe–Fe distance observed in the blue peroxodiferric complex of ferritin.

Introduction

The speed and complexity of Fe^{2+} oxidation at ferritin ferroxidase centers limit the direct structural data available about the intermediates involved. In fact, crystallographic data have been compiled for none of the iron complexes. The stable species on the reaction path must, however, be identified if the mechanism of the ferroxidase reaction is to be understood. Accurate density functional theoretical (DFT) calculations have been valuable in explicating mechanisms of reactions at diiron centers in other proteins, and it seems feasible that insight into the structures of complexes formed at the ferritin ferroxidase centers might be gleaned from such calculations, informed by indirect structural information available from the many kinetics and spectroscopic studies of the reaction. We have therefore constructed a six-amino acid model of the ferroxidase center in human H ferritin (HuHF), examined the structures of several Fe(II) and Fe(III) complexes that can be related to experimental observations, and used these to test how well the model site represents the known chemistry of the center.

Ferritins[1] are proteins within cells that bind Fe(II), oxidize it to Fe(III) oxide hydrate, and store it for later use. Ferritins of vertebrates are made up of 24 subunit proteins of two types, H and L. The subunits self-assemble into a hollow spherical structure[2] with an inner diameter of about 80 Å, providing storage capacity for more than 4000 iron atoms, and an outer diameter of about 120 Å. Each subunit consists of four parallel α-helices, A−D, running nearly the length of the protein plus a fifth short helix, E, and a loop connecting pairs of helices (see Figure 1a). H subunits contain a ferroxidase center at which Fe^{2+} is bound in pairs and oxidized by O_2 to an Fe(III) oxide hydrate. Ferritin sequence, folding, tertiary, and quaternary structures are highly conserved across plants and animals.

The mechanism of iron binding and oxidation at the ferroxidase centers in ferritin is known in outline. Iron ions enter the protein through one of several hydrophilic channels.[1,3] Entry seems to be impelled by an electrostatic gradient.[4,5] At the ferroxidase center of an H subunit Fe^{2+} ions are bound and oxidized pairwise by O_2 to a μ-1,2-peroxodiiron(III) complex, the one intermediate that is spectroscopically well characterized. The peroxodiferric complex is readily identified by its blue color ($\lambda_{max} = 650$ nm). Mössbauer and resonance Raman spectra place the complex structurally in the same class as the diiron(III)

* To whom correspondence should be addressed. E-mail: robert.binning@gmail.com. Fax: (787) 759-7663.
† Universidad Metropolitana.
‡ Universidad Nacional de la Patagonia San Juan Bosco.

(1) Liu, X.; Theil, E. C. *Acc. Chem. Res.* **2005**, *38*, 167.
(2) Banyard, S. H.; Stammers, D. K.; Harrison, P. M. *Nature (London)* **1978**, *271*, 282.
(3) Chasteen, N. D.; Harrison, P. M. *J. Struct. Biol.* **1999**, *126*, 182.
(4) Douglas, T.; Ripoll, D. R. *Protein Sci.* **1998**, *7*, 1083.
(5) Takahashi, T.; Kuyucak, S. *Biophys. J.* **2003**, *84*, 2256.

10.1021/ic060388k CCC: $33.50
Published on Web 11/16/2006

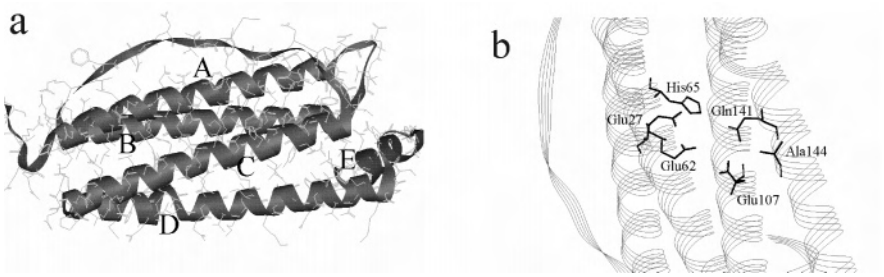

Figure 1. (a) Ribbon representation of a subunit of human H ferritin with helices A−E labeled. (b) Rotated HuHF subunit with the six amino acids that comprise the model ferroxidase center discussed in the text shown in black outline.

peroxides seen in enzymes, and the Fe−Fe distance in the bullfrog M ferritin complex (2.53 Å) has been determined by analysis of its extended X-ray absorption fine structure (EXAFS).[6] This complex decays, probably by hydrolysis, to at least one additional intermediate,[7,8] and eventually a hydrated iron (III) oxide is transported to the center cavity of the protein. The overall ferroxidase process may be written

$$2Fe^{2+} + O_2 \rightarrow [Fe^{3+}-O-O-Fe^{3+}] + (H_2O)_{x+3} \rightarrow Fe_2O_3(H_2O)_x + 4H^+ + H_2O_2 \quad (1)$$

Additional paths exist for Fe^{2+} oxidation in ferritin.[9] Product hydrogen peroxide from reaction 1 can oxidize Fe^{2+}, and once mineralization in the central cavity is underway, oxidation occurs at the mineral surface.[7] But reaction 1 is associated with the rapid oxidation of Fe^{2+} in H ferritin and is key to understanding its function.

Although ferrous ion binding has been intensely studied, bound Fe^{2+} has not been directly observed, owing to the rapidity of the oxidation and the fact that the product is transported from the site. Locating and defining the binding sites, usually designated A and B, occupied by two Fe^{2+} ions in the ferroxidase center has been a focus of study. In a broad sense X-ray crystallography of proteins cocrystallized with various cations has located the ferroxidase site, while combined kinetics, spectroscopy, and site-directed mutagenesis studies have refined the understanding of the essential amino acids involved. Cocrystallization of HuHF with Ca^{2+} and Tb^{3+},[10,11] bullfrog M (a variant of H) ferritin (FrMF)[12] with Mg^{2+}, and *Escherichia coli* conventional H ferritin (EcFTN)[13] with Fe^{3+} has located likely binding positions in X-ray crystal structures.[14] Site A has been clearly identified with three amino acids, the glutamate at position 27 (Glu27), Glu62, and a histidine, His65. The fact that this set of amino acids is consistently conserved in H ferritins (and not generally found in L[11]) argues in favor of the significance of the site. In addition the Glu, Glu-X-X-His pattern occurs in the diiron centers of several enzymes.[15] Site B has also been located, if not completely defined, by cocrystallization. Mg^{2+} clearly associates with Glu107, Gln141, and Asp144 in bullfrog M ferritin.[12] Cocrystallization of HuHF[10,11] is not as definite; among the difficulties are the facts that position 144 in HuHF is occupied by inert Ala, Glu62 may bridge sites A and B, and other residues can be interpreted as playing a role in the structure. Yet the general location of the site is not in question and corresponds with that seen in FrMF.

The active components of the ferroxidase center in human H and bullfrog M ferritins have been more precisely defined by a combination of site-directed mutagenesis, kinetics, and spectroscopy. In human H ferritin, mutation of residues Glu62 and His65 was found to eliminate binding of Fe^{2+},[16] whereas little effect was seen upon mutation of Glu61, Glu64, and Glu67. Liu and Theil[17] have defined the essential ferroxidase active site in FrMF. Introducing site B amino acids Glu107, Gln141, and Asp144 one-by-one into a bullfrog L ferritin in which the site A residues had already been incorporated, they observed the onset of ferrous oxidation and formation of the peroxodiferric complex. Neither the presence of site A alone nor of single Glu107, Gln141, or Asp144 substitutions affected activity. Introduction of all three site B amino acids resulted in a ferrous oxidation rate similar to that seen in wild-type ferritin, and formation of the peroxodiferric complex was observed. They therefore concluded that the components of the ferroxidase site in the M ferritin are a Glu, Glu-X-X-His site A and a Glu, Gln-X-X-Asp site B. Position 144 shows variation within and across species. In bullfrog H ferritin it is occupied by serine, in human H by alanine, and in EcFTN by glutamate. The other five positions involved in sites A and B, on the other hand, are conserved in all known H ferritins.

(6) Hwang, J.; Krebs, C.; Huynh, B. H.; Edmondson, D. E.; Theil, E. C.; Penner-Hahn, J. E. *Science* **2000**, *287*, 122.
(7) Bou-Abdallah, F.; Zhao, G.; Mayne, H. R.; Arosio, P.; Chasteen, N. D. *J. Am. Chem. Soc.* **2005**, *127*, 3885.
(8) Jameson, G. N. L.; Jin, W.; Krebs, C.; Perreira, A. S.; Tavares, P.; Liu, X.; Theil, E. C.; Huynh, B. H. *Biochemistry* **2002**, *41*, 13435.
(9) Bou-Abdallah, F.; Biasiotto, G.; Arosio, P.; Chasteen, N. D. *Biochemistry* **2004**, *43*, 4332.
(10) Hempstead, P. D.; Yewdall, S. J.; Fernie, A. R.; Lawson, D. M.; Artymiuk, P. J.; Rice, D. W.; Ford, G. C.; Harrison, P. M. The Protein Data Bank, 2FHA. *J. Mol. Biol.* **1997**, *268*, 424.
(11) Lawson, D. M.; Artymiuk, P. J.; Yewdall, S. J.; Smith, J. M. A.; Livingstone, J. C.; Treffry, A.; Luzzago, A.; Levi, S.; Arosio, P.; Cesareni, G.; Thomas, C. D.; Shaw, W. V.; Harrison, P. M. *Nature (London)* **1991**, *349*, 541.
(12) Ha, Y.; Shi, D.; Small, G. W.; Theil, E. C.; Allewell, N. M. *J. Biol. Inorg. Chem.* **1999**, *4*, 243.
(13) Stillman, T. J.; Hempstead, P. D.; Artymiuk, P. J.; Andrews, S. C.; Hudson, A. J.; Treffry, A.; Guest, J. R.; Harrison, P. M. *J. Mol. Biol.* **2001**, *307*, 587.
(14) Sequencing varies among ferritins; sequence numbering in this work follows that in HuHF (ref 10).
(15) Tshuva, Y.; Lippard, S. J. *Chem. Rev.* **2004**, *104*, 987.
(16) Bou-Abdallah, F.; Arosio, P.; Santambrogio, P.; Yang, X.; Janus-Chandler, C.; Chasteen, N. D. *Biochemistry* **2002**, *41*, 11184.
(17) Liu, X.; Theil, E. C. *Proc. Natl. Acad. Sci. USA* **2004**, *101*, 8557.

Diiron centers in proteins are not rare.[15] The Protein Data Bank lists structures of 17 distinct proteins that contain diiron centers. With the exceptions of the dioxygen transport protein hemerythrin[18] and ferritin, diiron centers occur in enzymes, where they activate dioxygen in a variety of reactions. The ferritin diiron center is unique in being a substrate that is eventually transported from the ferroxidase center, whereas in other proteins the diiron centers are catalytic cofactors. In methane monooxygenase (MMO) and Δ9-desaturase (Δ9D) the diiron center has double Glu, Glu-X-X-His groupings around the irons. The R2 subunit of ribonucleotide reductase (RNR) is similar, with one glutamate replaced by an aspartate. Each of these enzymes forms a peroxodiiron(III) complex with visible, Raman, and Mössbauer signatures similar to those seen in the ferritin diiron(III) peroxide complex, though the Fe−Fe distance in ferritin is shorter than in other diiron(III) centers.[6] In addition the ferritin diiron center resides in a hydrophilic region of the protein, whereas in the enzymes the surroundings are more hydrophobic, and radical mechanisms are important.[19] It has been argued[6] that the ferroxidase site may have evolved from a double Glu, Glu-X-X-His center, alterations in the site B amino acids being driven by the necessity for looser binding of the iron ion pair to facilitate release of the product oxide.

All-electron theoretical methods have been sparsely applied to ferritin. We[20] have applied DFT calculations to di-(μ-oxo)μ-1,2 peroxodiiron(III) complexes, Fe_2O_4 and $Fe_2O_4(H_2O)_6$, that may provide models for the ferritin peroxodiferric complex. Ciacchi and Payne[21] have performed DFT optimizations and molecular dynamics in exploring the regulation of O_2 entry into the ferroxidase site. Density functional theory has been extensively applied to the study of reaction mechanisms of the important RNR and MMO enzymes,[18,19,22−28] and it has been successful in identifying key intermediates and transition states. These systems have stable diiron(II) and -(III) intermediates for which crystallographic structures have been obtained, although in the case of RNR the diferric intermediate has been crystallographically defined for mutants that slow the reaction with O_2.[29] Theoretical studies have used these to construct and test models with which to search reaction paths.[23,30]

In the absence of crystal structures of ferritin iron complexes, exploration of the ferroxidase center must proceed by a somewhat different path than it has with the enzymes MMO and RNR, for which the atomic positions of diiron complexes are well defined. The picture of ferritin structure will have to be developed gradually, in a process that combines exploration of structures of iron complexes and incremental improvement in the representation of solvation and secondary amino acid effects. The initial question, and the one this study is concerned with, is whether a minimal model center consisting of amino acids at positions 27, 62, and 65 (site A) and 107, 141, and 144 (site B) alone will serve to bind the complete set of iron complexes that form in the ferroxidase center in a physically realistic manner. If so, then that model center may, with improvements, provide a basis for quantitative study of the ferroxidase reaction. If not, the basic model will have to be augmented with elements that do permit this basic function. The present study essays to assess, through a series of exploratory calculations, whether the minimal model adequately represents the ferritin center. We have optimized structures of a sequence of complexes, ranging from iron(II) to diiron(II) to several diiron(III) peroxides, formed by the six-residue model. While the structures of the complexes formed in the ferroxidase reaction are unknown, the optimized complexes can be compared with experimental evidence of complex formation in the ferroxidase center to understand some of their structural attributes.

Methods

Energies were obtained in BPW91 density functional theoretical calculations. BPW91 consists of Becke's 1988 gradient-corrected exchange functional[31] and the correlation functional of Perdew and Wang.[32] The BPW91 functionals have been found to perform well in studies of organometallic complexes[33] and in iron−oxygen clusters.[34] Numerical basis sets of double numerical plus polarization quality (DNP) were employed, and calculations were carried out with the Dmol^3 program.[35,36] We have previously obtained satisfactory structures of peroxides and iron complexes with BPW91/DNP calculations.[20] In geometry optimizations the amide-bonded atoms of the protein helix backbone were capped with hydrogens and fixed in their crystallographically determined positions.[10] All other atoms were allowed to float. The specifics of which atoms were fixed and which floated can be found in the Supporting Information. Each complex optimized consisted of about 100 atoms. The systems under study are generally open-shell systems, and these have been approached with unrestricted DFT calculations. Many diiron complexes, including the ferritin peroxodiferric intermediate, are overall low-spin systems with two antiferromagnetically coupled high-spin irons. We have approached these cases with localized spin density, broken symmetry,[23] calculations. The broken symmetry state is a spin-averaged state that provides a working approximation in the weak-coupling limit to the intrinsically multiconfigurational problem presented by this case. It has been argued that the low-

(18) Solomon, E. I.; Brunold, T. C.; Davis, M. I.; Kemsley, J. N.; Lee, S.-K.; Lehnert, N.; Neese, F.; Skulan, A. J.; Yang, Y.-S.; Zhou, J. *Chem. Rev.* **2000**, *100*, 235.
(19) Himo, F.; Siegbahn, P. E. M. *Chem. Rev.* **2003**, *103*, 2421.
(20) Bacelo, D. E.; Binning, R. C. *Int. J. Quantum Chem.*. **2005**, *105*, 740.
(21) Ciacchi, L. C.; Payne, M. C. *Chem. Phys. Lett.* **2004**, *390*, 491.
(22) Baik, M.-H.; Newcomb, M.; Friesner, R. A.; Lippard, S. J. *Chem. Rev.* **2003**, *103*, 2385.
(23) Noodleman, L.; Lovell, T.; Han, W.-G.; Li, J. *Chem. Rev.* **2004**, *104*, 459.
(24) Torrent, M.; Musaev, D. G.; Basch, H.; Morokuma, K. *J. Comput. Chem.* **2002**, *23*, 59.
(25) Gherman, B. F.; Lippard, S. J.; Friesner, R. A. *J. Am. Chem. Soc.* **2005**, *127*, 1025.
(26) Han, W. G.; Liu, T.; Lovell, T.; Noodleman, L. *J. Am. Chem. Soc.* **2005**, *127*, 15778.
(27) Skulan, A. J.; Brunold, T. C.; Baldwin, J.; Saleh, L.; Bollinger, J. M.; Solomon, E. I. *J. Am. Chem. Soc.* **2004**, *126*, 8842.
(28) Wei, P.; Skulan, A. J.; Wade, H.; DeGrado, W. F.; Solomon, E. I. *J. Am. Chem. Soc.* **2005**, *127*, 16098.
(29) Saleh, L.; Krebs, C.; Ley, B. A.; Naik, S.; Huynh, B. H.; Bollinger, J. M. *Biochemistry* **2004**, *43*, 5953.
(30) Siegbahn, P. E. M. *Q. Rev. Biophys.* **2003**, *36*, 91.
(31) Becke, A. D. *Phys. Rev. A* **1988**, *38*, 3098.
(32) Perdew, J. P.; Wang, Y. *Phys. Rev. B* **1992**, *45*, 13244.
(33) Stöckigt, D. *Organometallics* **1999**, *18*, 1050.
(34) Gutsev, G. L.; Mochena, M. D.; Bauschlicher, C. W. *Chem. Phys. Lett.* **2005**, *407*, 180.
(35) Delley, B. *J. Chem. Phys.* **1990**, *92*, 508.
(36) Delley, B. *J. Chem. Phys.* **2000**, *113*, 7756.

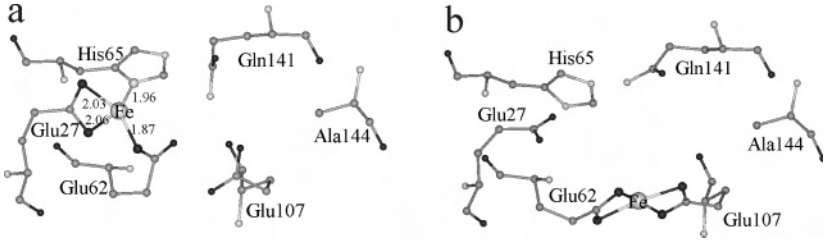

Figure 2. (a) Optimized structure of Fe^{2+} ion bound in site A of the model center, composed of His65, Glu27, and Glu62. (b) Fe^{2+} bound by Glu62 and Glu107 in site B′. Oxygen atoms are black, carbons darker gray, and nitrogens lighter gray. Hydrogen atoms have been omitted. Distances are in angstroms.

spin antiferromagnetic case is better treated as a high-spin system.[24] The high-spin state can be represented as a single configuration, and because coupling between centers is weak, the error should be small. In fact the structural differences in dimetal complexes arising from the two methods have not been thoroughly examined. The conclusions sought in this study are essentially qualitative and unlikely to be affected by our choice.

Results and Discussion

The location of the ferroxidase site in the first subunit of HuHF (coordinates taken from ref 10) is illustrated in Figure 1b. Glu27 on helix A, Glu62 and His65 on helix B, Glu107 on helix C, and Gln141 and Ala144 on helix D are shown in outline. Glu27, Glu62, and His65 form a natural pocket for a cation that has been identified as site A of the ferroxidase center.[1,11] Glutamic acid is deprotonated near neutral pH. Histidine is neutral, but imidazole to imidazolium protonation occurs between pH 6 and 7, and the kinetics of ferrous ion binding are seen to change in that range.[16] Glu107 on helix C and Gln141 and Ala144 on helix D comprise site B of the model center. The model excludes water molecules. The ferroxidase center resides in a hydrophilic region, and this omission is therefore physically unrealistic, but it confers the advantage of emphasizing the primary ligand−metal interactions in the optimized iron and diiron complexes.

The initial set of optimizations examined the binding of Fe^{2+} at sites A and B. Figure 2a displays Fe^{2+} at site A. Fe^{2+} placed near Glu27 and Glu62 and the imidazole group of His65 moved into the site during optimization. It is tetracoordinated to the three ligands; Glu27 is bidentate. Bidentition by Glu27 is consistent with, though not definitely confirmed by, its orientation in crystal structures near Mg^{2+} of FrMF[12] and Tb^{3+} in HuHF.[11] The iron−nearest atom distances, ranging from 1.96 to 2.06 Å, indicate strong bonding, and the gross atomic charges from population analysis of about −0.5 on proximal O and N and +0.75 on Fe indicate ionic bonding, but with significant charge transfer. The optimized structure of the iron complex therefore concurs with previously postulated structures based on crystallographic evidence.[11,12]

Fe^{2+} placed near site B did not bind there but migrated to lodge between the carboxylates of Glu107 and Glu62 in the structure shown in Figure 2b. We may call this site B′; it is about 5 Å from site A. The failure to occupy site B is consistent with observations on HuHF[37] that site B is not occupied by Fe^{2+} until site A is. Both complexes shown in Figure 2 are in well-defined triplet, intermediate spin, states. While high-spin Fe^{2+} is to be expected, it may be seen that in both complexes the metal is approximately square-planar coordinated in the absence of solvent molecules, and in this environment the triplet state is reasonable. It must also be noted that the electronic states of iron(II)-ferroxidase complexes have not been determined.

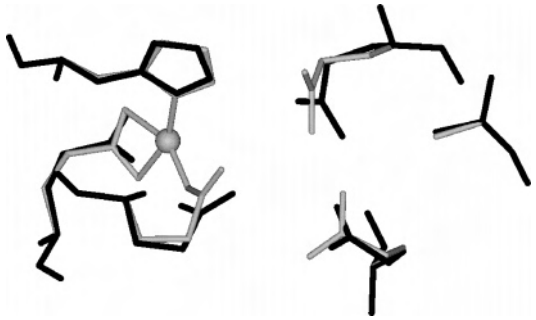

Figure 3. Original atomic positions of six amino acids (in black, ref 10) superimposed on the optimized structure of Fe^{2+} bound at site A (gray) from Figure 2a.

Figure 3 shows the optimized structure of Figure 2a superimposed on the original crystallographic positions of the atoms of the model site. It illustrates the geometric changes that accompany binding of Fe^{2+} at site A. The changes are rather modest, involving primarily twisting of the glutamates and glutamine to orient their oxygens toward iron. Histidine is displaced very little.

A diiron(II) complex is generally believed to be precursor to the ferritin peroxodiiron(III) complex. Zn^{2+} in EcFTN[13] and Mg^{2+} in FrMF[12] form dication centers, and kinetics studies on HuHF[37,38] indicate that two Fe^{2+} ions are in place when rapid oxidation takes place. The next complexes to be optimized were therefore diiron(II) structures (Figure 4) derived by adding an Fe^{2+} to each of the complexes of Figure 2. We should note that a calorimetric titration study of Fe^{2+} binding to HuHF[16] has indicated that only one Fe^{2+} binds strongly to the ferroxidase center in the absence of dioxygen. Thus the assumption that a diiron structure is in place before oxidation is reasonable but not established; oxidation may be stepwise, and it is possible that the diiron center does not form until O_2 is present.

Inserting a second Fe^{2+} into the structure of Figure 2a, directed from site A toward Glu107 and Gln141, led to the optimized structure shown in Figure 4a. In the studies that

(37) Treffry, A.; Zhao, Z.; Quail, M. A.; Guest, J. R.; Harrison, P. M. *Biochemistry* **1997**, *36*, 432.

(38) Bauminger, E. R.; Harrison, P. M.; Hechel, D.; Hodson, N. W.; Nowik, I.; Treffry, A.; Yewdall, S. J. *Biochem. J.* **1993**, *296*, 809.

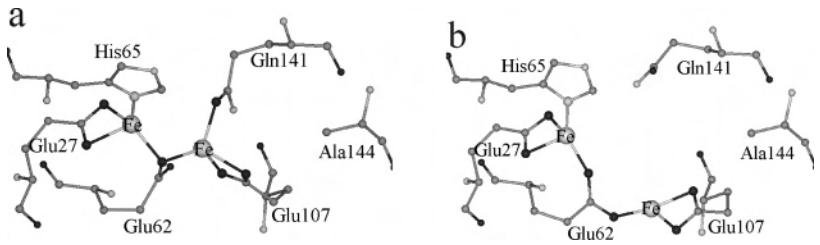

Figure 4. (a) Optimized structure of the complex formed when a second Fe^{2+} is added to the structure shown in Figure 2a. The second Fe^{2+} is bound at site B. (b) Complex formed by addition of a second iron(II) to the Figure 2b structure.

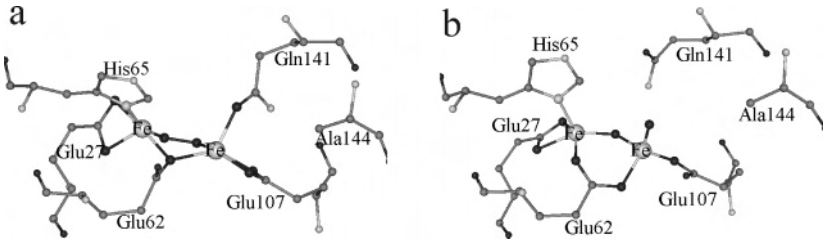

Figure 5. (a) Diiron(III) peroxide complex resulting from insertion of O_2 into the structure of Figure 3a and subsequent optimization. (b) A diiron(III) dioxide resulting from optimization of O_2 inserted into the structure of Figure 3b.

find evidence of diiron(II) complex formation, site A is observed to be occupied before site B;[37] the construction of Figure 4a is congruent with that sequence. The Fe−Fe separation is 3.28 Å, and the two irons are carboxo bridged by Glu62 (we use the term "carboxo" to indicate bridging by only one carboxylate oxygen, distinguishing it from "carboxylato" bridging by both oxygens). Whereas a single iron ion failed to bind at site B, with another iron at site A, binding does occur there. When site A is occupied, one oxygen of Glu62 is coordinated to the iron there and is thus not available to an iron at site B′, and site B becomes preferred to B′. Both irons are approximately tetrahedrally coordinated, whereas in the single-ion structures of Figure 2, coordination around each Fe^{2+} is nearly planar. The metals in each of the Figure 4 complexes are high-spin with antiferromagnetic coupling, so that the complex as a whole is in a singlet state. This is the electronic configuration in most reduced diiron intermediates, although the high-spin case is certainly seen.[39]

Carboxo bridges are found in diiron complexes,[15,40] but carboxylato bridging by Glu62 is perhaps more to be expected because the enzyme diiron centers are carboxylate bridged, and the ferritin complexes are usually classed with these.[15,41] In addition the position of the Glu62 carboxylate seems to bridge Zn^{2+} and Fe^{3+} ions in EcFTN[13] and Mg^{2+} ions in FrMF.[12] However, it has been hypothesized that the short Fe−Fe distance seen in the ferritin peroxodiferric complex precludes carboxylate bridging,[6] and in fact carboxo bridging is consistent with the positions of Glu62 seen in cocrystallized HuHF structures.[10,11]

The starting configuration for the optimized structure shown in Figure 4b was derived from that of Figure 2b by extending a second Fe^{2+} toward His65 and Glu27, in the direction of site A. During optimization the added ferrous ion moved more than 2 Å into the site A pocket. The resulting structure does exhibit a carboxylate bridge, but the Fe−Fe distance is 4.97 Å. Although one Fe^{2+} migrates into site A, the second remains in its initial position (see Figure 2b). The structure of Figure 5a is 2.5 kcal/mol more stable than that of Figure 4b, but the large geometric difference between the two configurations should inhibit interconversion.

The diferrous complex is oxidized by O_2 to the spectroscopically observed ferritin peroxodiiron(III) complex.[17,41] The spectroscopically characterized intermediate probably also possesses at least one oxo or hydroxo bridge, and these may well be present before the peroxide is formed. However, in Figure 5a we see a diiron(III) peroxide complex derived by simply inserting O_2 into the structure of Figure 4a, parallel to the Fe−Fe line and displaced to one side, followed by optimization. A peroxide bridge forms (Figure 5a), and the carboxo Glu62 bridge remains intact. The Fe−Fe distance in the complex, 3.17 Å, is shortened but still longer than that observed in the peroxodiferric complex.

Insertion of O_2 between the two iron ions of Figure 4b yields the complex shown in Figure 5b. Initial placement of O_2 directly along the Fe−Fe line was indicated due to the long Fe−Fe distance. Here a peroxide bridge does not form, rather O_2 forms an oxide and an oxo bridge. We have noted in calculations on Fe_2O_4 complexes[20] that the peroxide bridge is actually a local minimum structure, and that structures in which the O−O bond is sundered are lower in energy. The great distance between the iron ions in the starting structure for the optimization may bar access to the portion of the potential surface in which the peroxide bond is stable. An occupied site B seems to be needed to bring the two metals close enough for the peroxide to form. The oxo bridge that does form brings the irons about as close together, 3.2 Å, as they are in the complex of Figure 5a.

(39) Siegbahn, P. E. M. *Inorg. Chem.* **1999**, *38*, 2880.
(40) Chen, W.-H.; Wei, H.-H.; Lee, G.-H.; Wang, Y. *Polyhedron* **2001**, *20*, 515.
(41) Moënne-Loccoz, P.; Krebs, C.; Herlihy, K.; Edmondson, D. E.; Theil, E. C.; Huynh, B. H.; Loehr, T. M. *Biochemistry* **1999**, *38*, 5290.

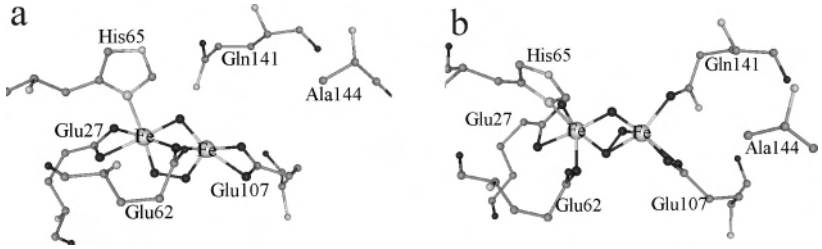

Figure 6. (a) Optimized structure resulting from addition of an oxide bridge to the structure shown in Figure 4a. (b) A structure derived by rotation of the core structure along the Fe−Fe axis, with subsequent optimization.

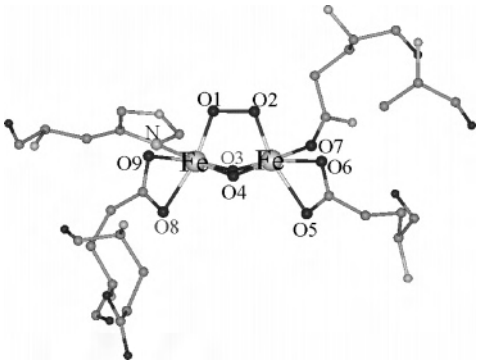

Figure 7. A di(μ-oxo)μ-1,2-peroxodiiron(III) complex of the type proposed in ref 6 as a model for the spectroscopically observed ferritin peroxodiferric complex.

Thus in the presence of dioxygen the complex of Figure 4a is converted into a peroxodiferric complex. The complex depicted in Figure 5a is stable, but it is not a successful model for the ferritin diiron(III) peroxide complex because the Fe−Fe distance is too long. It has been suggested that the short Fe−Fe distance is the result of oxo or hydroxo bridging, which may originate as hydrate bridges.[6,17] Consequently, into the open coordination positions of the structure seen in Figure 5a we inserted an oxide. The bridge is stable, and the structure of the resulting complex is shown in Figure 6a. The Fe−Fe distance in this complex is 2.76 Å, slightly[8] too long for the peroxodiiron(III) intermediate of ferritin. However, the structure has a hydrogen bond (H···O bond length 1.65 Å) from the neighboring Gln141 to the oxo bridge, and this may affect the Fe−Fe distance.

Changing the initial position of the bridging oxide in the structure of Figure 5a resulted in the complex shown in Figure 6b. It is an asymmetric structure in which the Glu62 carboxylate has shifted so that it is no longer a bridging ligand, and the peroxide bridge also changes form. This type of structure has been previously optimized in a search for a diiron(III) intermediate in the activation of O_2 in the enzyme MMO.[42] That intermediate was found to lie higher in energy than a symmetric nonplanar bridging μ-η^2:η^2 "butterfly" configuration. We did not locate a butterfly configuration in the limited number of optimizations this study permitted.

We constructed one other model, incorporating two simple oxo bridges rather than the oxo-carboxo bridge seen in Figure 6a. The core di(μ-oxo)μ-1,2-peroxodiiron(III) structure of this complex was proposed by Hwang et al.[6] to account for the short Fe−Fe distance in the peroxodiferric complex of ferritin. We have previously optimized similar Fe_2O_4 structures.[20] The Fe_2O_4 core fits easily into the model active site, and the optimized structure seen in Figure 7 results. Table 1 lists in detail the bond lengths and angles that define the diiron center. Glu62 is coordinated to neither iron in this complex, and alternative structures in which it participates are obvious candidates for further exploration. The Fe−Fe distance of 2.65 Å is more than 0.1 Å longer than the experimentally derived distance of 2.53 Å, but may well lie within the combination of experimental uncertainty and the error in the calculated structure, and the complex of Figure 7 is thus a potentially successful model for the ferritin intermediate. Besides double μ-oxo bridging, the "carboxylate-shift" to a μ-1,2-carboxylate bridge has been postulated[43] as a potential structural element that may shorten Fe−Fe distances, and this mechanism deserves to be examined.

Conclusions

The six-residue model examined in this study successfully mimics basic functions observed in the HuHF ferroxidase center. It binds Fe^{2+}, singly and in pairs, in physically reasonable positions. The second iron binds at site B provided site A is first occupied, in accord with observed behavior. The model diiron(II) center forms a peroxide with dioxygen, and it forms diiron(III) peroxide complexes. A stable di(μ-oxo)μ-1,2-peroxodiiron(III) complex forms, is bound in the model center and displays a short Fe−Fe separation, a distinctive feature of the spectroscopically observed ferritin peroxodiiron intermediate. These complexes form without

Table 1. Selected Distances and Angles Defining the Diiron(III) Center Shown in Figure 7

		Bond Distances (Å)			
Fe···Fe	2.643	O1−O2	1.429	Fe−O3	1.816, 1.821
Fe−O4	1.829, 1.842	Fe−O5	2.224	Fe−O6	2.173
Fe−O7	2.085	Fe−O8	2.166	Fe−O9	2.148
		Fe−N	2.236		
		Bond Angles (deg)			
Fe−O−O−Fe	2.18	Fe−O1−O2	109.06	O1−Fe−O3	89.34
O1−Fe−N	84.95	O3−Fe−O4	80.86	O2−Fe−O5	162.74
O2−Fe−O6	102.39	O2−Fe−O7	92.76	O5−Fe−O6	60.50
O8−Fe−O9	61.70	N−Fe−O8	91.07	N−Fe−O9	93.92

assistance from neighboring amino acid residues and without accommodative changes in secondary structure, although each of these may certainly play a role in the dynamics of the overall reaction.

Therefore the minimal six-amino acid model under examination does provide a basis for more thorough study of the structures and energetics of iron complex intermediates similar to those that occur in the ferroxidase reaction. Ala144 is inert and sterically unimportant in the optimizations carried out in this study, so it may be excluded from the model of HuHF. The survey of complexes raises questions at each step, but the broad approach provides an overall qualitative comparison of the model complexes with available experimental evidence. Additions to this model of solvent structure, counterions, and perhaps some secondary amino acid residues should permit accurate calculation of the structures and energetics needed to understand this important system.

(42) Gherman, B. F.; Baik, M.-H.; Lippard, S. J.; Friesner, R. A. *J. Am. Chem. Soc.* **2004**, *126*, 2978.
(43) Torrent, M.; Musaev, D. G.; Morokuma, K. *J. Phys. Chem. B* **2001**, *105*, 322.

Acknowledgment. R.C.B. gratefully acknowledges support from the U.S. National Institutes of Health (NIH) through UMET-OSBRA 1G11HD046374-01, and D.E.B. acknowledges support from the Consejo Nacional de Investigaciones Científicas y Técnicas de la República Argentina.

Supporting Information Available: Computational details and complete Cartesian coordinate files in XYZ format for the optimized complexes illustrated in Figures 2−7. This material is available free of charge via the Internet at http://pubs.acs.org.

IC060388K